







Dune dynamics in the southern edge of Dunhuang Oasis and implications for the oasis protection

AN Zhi-shan^{1,2}  <http://orcid.org/0000-0003-0262-4717>; e-mail: an1986wen@163.com

ZHANG Ke-cun^{1,2*}  <http://orcid.org/0000-0003-3270-2843>;  e-mail: kecunzh@lzb.ac.cn

TAN Li-hai^{1,2}  <http://orcid.org/0000-0001-7727-9722>; e-mail: tanlihai18@163.com

ZHANG Hu³  <http://orcid.org/0000-0002-2580-4326>; e-mail: 526256421@qq.com

NIU Bai-cheng^{1,2}  <http://orcid.org/0000-0002-4962-5998>; e-mail: 707481314@qq.com

*Corresponding author

¹ Dunhuang Gobi and Desert Research Station, Northwest Institute of Eco-Environment and Resources, Chinese Academy of Sciences, Lanzhou 730000, China

² Key Laboratory of Desert and Desertification, Chinese Academy of Sciences, Lanzhou 730000, China

³ Academy of Water Resource Conservation Forests of Qilian Mountains in Gansu Province, Test Station of Desertification Control in Hongshawo, Zhangye 734000, China

Citation: An ZS, Zhang KC, Tan LH, et al. (2018) Dune dynamics in the southern edge of Dunhuang Oasis and implications for the oasis protection. *Journal of Mountain Science* 15(10). <https://doi.org/10.1007/s11629-017-4723-2>

© Science Press, Institute of Mountain Hazards and Environment, CAS and Springer-Verlag GmbH Germany, part of Springer Nature 2018

Abstract: The survival of Dunhuang Oasis is largely determined by the evolution of sand dunes in the southern edge of the oasis, mainly composed of shield dunes and mega pyramid dunes, which occupy two-thirds and one-third of the area, respectively. However, few studies have focused on dynamics of these dunes, especially in terms of quantification. So the theoretical basis of sand-control engineering is relatively limited. Here we present the characteristics of dune dynamics of a shield dune and mega pyramid dune in the southern edge of Dunhuang Oasis during April 2014–April 2016 based on measurement data of a 3-D laser scanner. Results indicate that the volume of the shield dune decreased during the monitoring period of two years, and the gravity centers of the monitored shield dune moved windward, indicating that sand was transported toward the oasis. Conversely, the dune volume of the mega pyramid dune increased and the gravity center presented no prominent movement, indicating that the mega

pyramid dune was relatively stable and its migration toward the oasis was not notable. Thus, compared with mega pyramid dunes, shield dunes in the southern edge of Dunhuang Oasis are identified as a more significant sand source endangering the protection of the oasis, and sand-control engineering should mainly focus on these shield dunes.

Keywords: Dunhuang Oasis; Dune dynamics; 3-D laser scanner; Shield dune; Mega pyramid dune

Introduction

Desert and oasis are the most typical surface landscapes in arid regions. Although the oasis only accounts for 4% of the total area of arid regions, it brings up a population of more than 95% and creates brilliant ancient civilization (Wang et al. 2012; Zhang and Dong 2015). Desert and oasis coexist with mutual interaction. The desert acts as one of major sources of wind-blown sand activities,

Received: 16 October 2017
Revised: 15 February 2018
Accepted: 30 August 2018

and dune migration is an important potential threat to the existence of the oasis. An effective way to combat dune migration and maintain the stability of oasis in arid regions is to establish an integrated sand control system including engineering and biological sand control measures at the edge of oasis (Liu et al. 2011; Ma et al. 2010; Qu et al. 2014; Tan et al. 2016; Zhang et al. 2014). Functioning as a barrier to reduce the pressure imposed by desert on oasis, the sand control system is able to effectively prevent desert expansion and dune migration from endangering the existence of oasis.

However, the edge between desert and oasis is a belt with weak ecological environment due to the complicated impact both from desert and oasis, and it is extremely sensitive to external condition changes (Huang et al. 2015; Ma et al. 2010; Mao et al. 2014a; Yong et al. 2007). Human activities will easily break the stability between oasis and desert and lead to various types of disasters such as land degradation and faster dune movement (Huang et al. 2015; Yong et al. 2007). So the establishment of an integrated sand control system at the oasis edge should be careful. The characteristics of the dune dynamics, such as the migration rate of different types of sand dunes and the temporal variation of dune morphology, are important theoretical basis to the integrated sand control system. Thus, the study on dune dynamics at the oasis edge can provide significant theoretical basis to the protection of oasis from wind-blown sand disasters.

As an ancient way station along the Silk Road in western China, Dunhuang is facing such the problem since it is surrounded by the Mingsha Mountain (dune field) to the south. Many integrated sand control systems have been established around the southern edge of Dunhuang Oasis such as those at the Mogao Grottoes (40°5'17.25"N, 94°40'16.67"E) and Crescent Moon Spring (40°5'11.98"N, 94°40'9.997"E) (Figure 1). To protect these heritages against sand drift, 18365 ha of shelterbelts (trees and shrubs) were established by local governments and the management departments in the 1950s, and more since the 1980s (Pang et al. 2014; Qu et al. 2014). However, the design principle of integrated sand control systems is mainly based on the protective effect of sand control measures (Ma et al. 2010). Although the protective mechanism of these

measures is revealed (Tan et al. 2014; Tan et al. 2016; Zhang et al. 2014; Zhang and Dong 2015), some protection system has lost their effectiveness as the change of time. The main reason is that the mechanism of these measures is based on results from wind tunnel tests or numerical simulations and more consideration is given to how to maximize the protective effect of these measures in a short time, lacking the observation on dune dynamics of different dune types in the southern edge of Dunhuang Oasis (Pang et al. 2014; Zhang et al. 2013). Therefore, systematic studies should be carried out urgently on the dune migration and the temporal variation of dune morphology.

In this study, a 3-D laser scanner is adopted to perform studies on dune dynamics of a shield dune and mega pyramid dune in the southern edge of Dunhuang Oasis during the period of April 2014-April 2016, aiming to provide scientific evidence to the protection of Dunhuang Oasis from wind-blown sand and dune migration.

1 Study Area and Methods

1.1 Study area

The study area—Mingsha Mountain extends from southwest to northeast for approximately 40

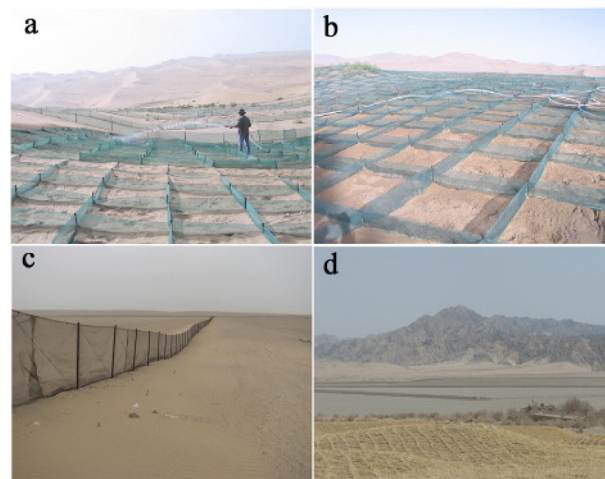


Figure 1 Sand control systems in the southern edge of Dunhuang Oasis. (a) and (b) are the protective measures including nylon checkerboard and sand fence in the Heishanzui area at the southern edge of Dunhuang Oasis; (c) and (d) are the protective measures atop the Mogao Grottoes at the southeast edge of Dunhuang Oasis, including a high sand fence with 'A' shape and straw checkboard.

km with a width of 15 km, located approximately 5 km south of the Dunhuang city, which is a famous historical and cultural city in Gansu Province, China. Within such a range, tall and compound mega pyramid dunes are widely distributed. The terrain inclines downward from south to north and is covered by aeolian landforms such as pyramid dunes, linear dunes and shield dunes. There are two major dune types in the southern edge of Dunhuang Oasis: one is shield dune, the other is mega pyramid dune. Shield dunes, with a shield shape, low height and an obvious slip face, are in the initial phase of the barchans, accounting for two-thirds of the study area. Mega pyramid dunes, with a shape like the pyramid in Egypt, a large height over 80 m and three or more arms/faces, accounts for one-third of the study area (Figure 2). Sands on the desert surface are dominated by medium sands; in comparison, on the surface of the oasis edge area, fine sands play a dominant role. As for natural vegetation in this region, it is rather monotonous and mainly covered by Sacsaul trees combined with *Nitraria tangutorum* Bobr and *Agriophyllum squarrosum* (L.) Moq., distributing sporadically in the study area.

The survey region of the shield dune is situated at the southwestern edge of Dunhuang

Oasis, and the length, width and height of the dune are approximately 70 m, 32 m and 1 m, respectively. The monitored mega pyramid dune, which has a relative height of 90 m, is located at the northern edge of the Mingsha Mountain dune field and in the north of the Crescent Moon Spring. This mega pyramid dune has three arms radiating from the central peak and extending to the north (5°), southeast (140°), and southwest (250°). The two adjacent arms constitute the E, S, and WNW dune sides. The E-facing side is a typical avalanche face at slope angles of 25°–32° with length of 386 m, and there is a gently sloping plinth ahead of this side. The S- and WNW-facing sides have respective slope angles of 25°–30° and 20°–30° and slope lengths of 266 and 209 m (Figure 2).

1.2 Methods

Possibilities of application of 3D laser scanning methods in polar conditions were tested by means of a Leica Scan station C10 scanner. The core working principle of this apparatus is the three-dimensional laser scanning technique, that is, a theory of laser ranging is utilized to collect three dimensional data of various large entities and real scenes into a computer completely through

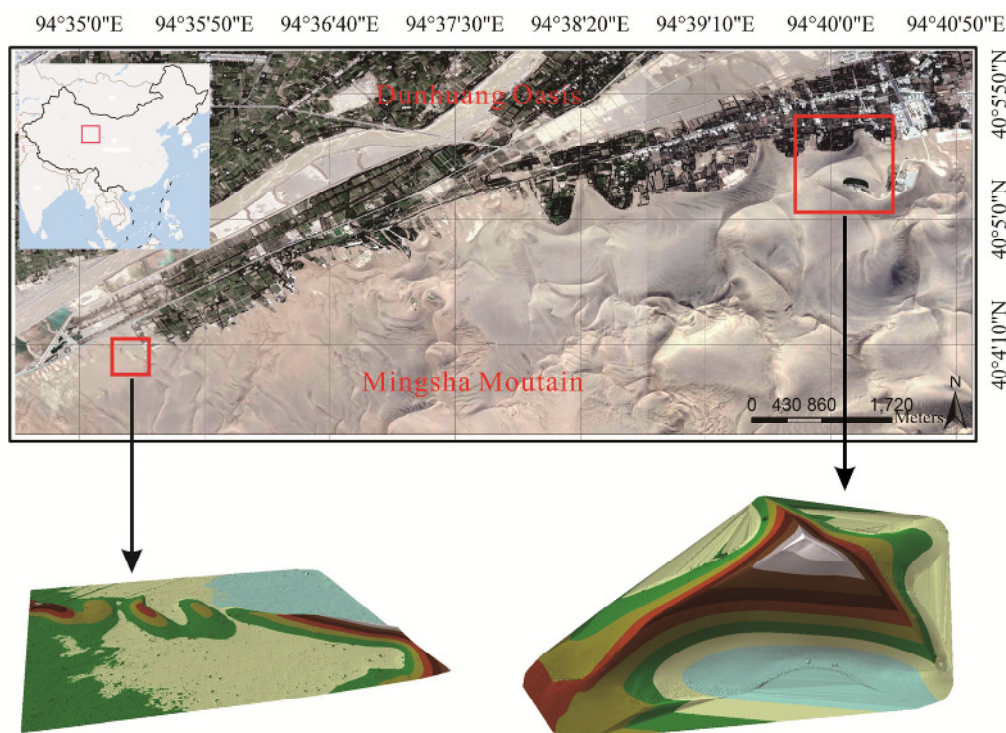


Figure 2 Location map of the study area and the monitored shield dune and mega pyramid dune.

recording three-dimensional coordinate and reflectance information of crowded surface points. Hence, the three-dimensional model including lines, planes and volumes of the measured object can be established in a rapid manner. Operation of the scanner model tested is based on stationary distance laser measurement with a rate of 50000 pt.s⁻¹, by means of a green pulse laser with a wavelength of 532 nm, and with a maximum measurable distance of 300 m reflectivity. The scanning geometry of Leica Scan Station C10 (up to 360° horizontally and up to 270° vertically) permits the measurements be performed in almost any terrain conditions. This device can operate in the temperature range of 0°C-40°C.

Topographic data acquisition can be divided into two parts which include field operations and indoor work. To be specific, field operations were carried out in respective April 5, 2014, April 5, 2015 and April 5, 2016 to lay control points and achieve data. Firstly, not only control points were laid within the survey region, but a local coordinate system was established, so as to guarantee that the scan data were within an identical coordinate system. Secondly, the 3-D laser scanner was used to perform multi-station scanning for the survey region. Specifically, the density of scanned data set was 10 cm×10 cm, automatic exposure served as the photo format of the built-in digital camera with a capacity of 5MP, the mosaic method among multiple stations was sphere target joint and 4 sphere targets were set between two stations to control the corresponding error no more than 6 mm. So data obtained in the form of a point cloud constitute a 'model space' with an accuracy of distance from the point location of up to 8 mm.

The principal indoor work is post processing of data, which includes joint, optimization and output of point cloud data. The last step is transforming into a digital terrain model. Data joint refers to a mathematical calculation process in which three-dimensional space data from multiple coordinate systems are converted into a uniform coordinate system. Such an operation must be accomplished by the "Cyclone 8.0" software package (<http://hds.leica-geosystems.com>).

Data optimization refers to the elimination of point cloud data irrelevant to the research object as well as the point cloud integration and simplification. By getting rid of mistaken points and gross error

points from the original point cloud data, initial characteristics of the object can be restored to improve the signal-to-noise ratio of data. Such a work procedure can also be fulfilled by the 'Cyclone 8.0' software package, while latter data optimization and graphic output are both completed by the software of ArcGIS 9.3. The detailed procedures are as follows. After improving the signal-to-noise ratio of data, we export the selected point cloud to text file including the x, y and z information with the precision better than 8 mm. Opening the text file with ArcGIS 9.3 and show all the point in the screen. Then convert the point text file into SHP file and create the Triangulated Irregular Network (TIN) on the basis of the SHP file. The final step is creating the Raster Data Model and calculating the width, length, height, basal area and volume of dune.

To calculate the dune volume, we used the volume module. This module calculated volume by summing cell values within a given area and the multiplying by area occupied by those cells. An elevation of 0 m (zero) was a reference base level and the area of the base level was defined as basal area. By virtue of variety of wind direction in the research area, we defined the width and length just considering the dune morphology rather than the prevailing wind direction. Finally, the height of the dune was defined at the highest point above the base level.

A HOBO U30 weather station in the study area was set up to measure wind speed, wind direction, temperature and air humidity. The height of wind speed sensor and wind direction sensor was 2 m above the ground. The height of temperature sensor and air humidity sensor was 1.5 m above the ground. The data acquisition time interval was 10 min.

2 Results

2.1 Sand-driving wind

During the observation period of 2014-2015, sand-driving winds mainly included three main directions, namely, southwest wind (SW, WSW and W), southeast wind (SE, SSE and S) and northeast wind (NNE, NE and ENE), which accounted for 43.79%, 29.27% and 20.68% of the total sand-

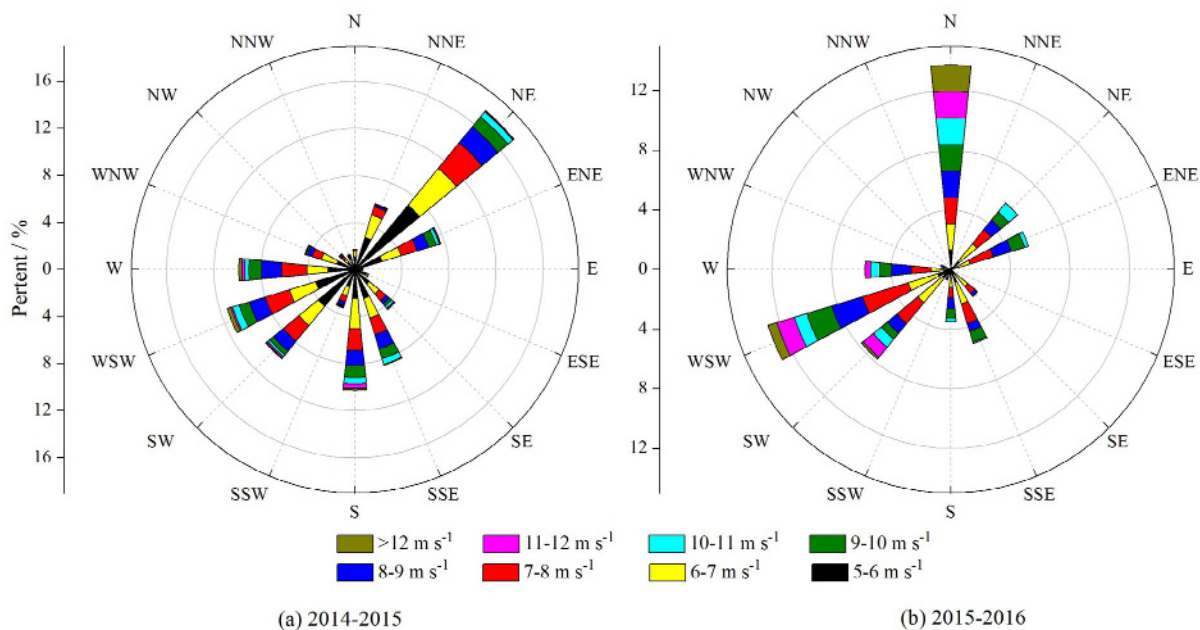


Figure 3 (a) Rose of sand-driving winds in the southern edge of Dunhuang Oasis in the period of 2014-2015. (b) Rose of sand-driving winds in the southern edge of Dunhuang Oasis in the period of 2015-2016.

Table 1 Morphological parameters of the shield dune in different monitoring periods

Period	Length (m)	Width (m)	Height (m)	Basal area (m ²)	Volume (m ³)	Displacement (m)	Direction
2014	69.51	32.15	1.06	1779.4	1076.01	3.45	NE32.9°
2015	70.99	32.7	1.01	1799.06	1013.34		
2016	71.7	31.6	1.14	1884.28	982.16		

driving winds, respectively. Therefore, the WSW wind accounted for 19.53% of all the sand-driving frequency. The sand-driving wind speed was mainly in the range of 5-8 m·s⁻¹, which accounted for 91.53% of all the sand-driving frequency. The directions of the maximum wind speed range (above 12 m·s⁻¹) mainly centralized in SW, WSW and W (Figure 3a).

The three main wind directions in the observation period of 2015-2016 were the same as those in the period of 2014-2015, including southwest wind (SW, WSW and W), southeast wind (SE, SSE and S) and northeast wind (NNE, NE and ENE), which accounted for 31.06%, 23.16% and 31.02% of the total sand-driving winds, respectively. There was also different in characteristics of wind regime between the period of 2015-2016 and 2014-2015. First, the proportion of NE sand-driving wind increased to 17.49% from 13.01% and the proportion of WSW sand-driving wind decreased to 11.36%. Second, the main range of sand-driving wind speed changed from 5-8 m·s⁻¹

into 5-10 m·s⁻¹, accounting for 94.05% of all the sand-driving frequency (Figure 3b).

2.2 Dune dynamics of shield dunes.

During the monitoring period of 2014-2015, all the length, height, and volume of the shield dune decreased, while its width and basal area increased (Table 1). As for the gravity center of the shield dune, it moved towards NE (32.91°) on the whole with a displacement distance of 3.45 m (Figure 4). Wind is the driving force for the migration of sand dunes. According to the calculation method of sand drift potential reported by Fryberger and Dean (1979), the sand drift potential above 10 m·s⁻¹ in the study area was 6.81VU, and the resultant drift potential was 1.37 VU with a resultant direction of 35.2°, which was consistent with the migration direction of the shield dune.

In the period of 2015-2016, the volume of the shield dune also decreased, but the width decreased, which was relatively contrary to the

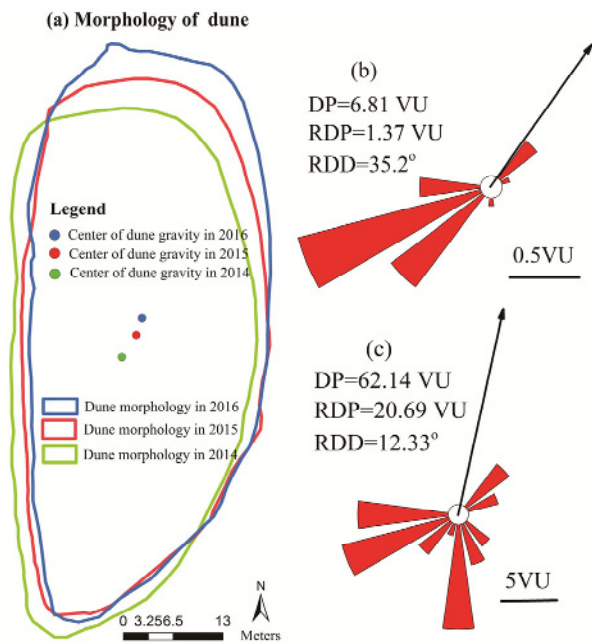


Figure 4 (a) Variation of the morphology of the monitored shield dune (the reference dune surface with a relative height of 0 m) in the monitoring period. (b) Sand drift potential rose above $10 \text{ m}\cdot\text{s}^{-1}$ during 2014-2015 period. (c) Sand drift potential rose above $10 \text{ m}\cdot\text{s}^{-1}$ during 2015-2016 period.

variation in 2014-2015. The dune length, height and basal area also increased. The annual sand drift potential above $10 \text{ m}\cdot\text{s}^{-1}$ was 62.14 VU , and the resultant drift potential was 20.69 VU with a resultant direction of 12.33° . The gravity center of the shield dune moved toward NE (19.7°), mainly consistent with the resultant direction.

Based on Figure 5a, the dune surface eroded by wind occupied a proportion of 51.54% for total area (2560 m^2) of the shield dune during 2014-2015, and the corresponding wind erosion amount was 8858.6 m^3 . Moreover, areas exposed to wind erosion were mainly distributed on the west side of the dune with a maximum wind erosion depth of 1.23 m, which occurred on the top of the dune. Sand deposition took a percentage of 48.46%, mainly distributing on the eastern area of the dune. The largest deposition thickness was 1.31 m which was greater than the maximum wind erosion depth,

and the total sand deposition quantity reached 8811.9 m^3 . Thus, sand materials of 46.7 m^3 from the shield dune were eroded during the observation time, and the annual erosion rate was $0.02 \text{ m}^3\cdot\text{m}^{-2}\cdot\text{yr}^{-1}$.

In the period of 2015-2016 (Figure 5b), the proportion of wind erosion surface area increased to 58.76% for total area (2560 m^2) of the shield dune, and the corresponding wind-erosion amount was 8652.7 m^3 . The dune surface in deposition took a percentage of 41.24%, and the deposition amount was 8599.89 m^3 . Sand materials of 52.81 m^3 from the shield dune were eroded in this year, and the annual erosion rate was $0.02 \text{ m}^3\cdot\text{m}^{-2}\cdot\text{yr}^{-1}$.

2.3 Dune dynamics of the mega pyramid dune

During 2014-2015, the monitored pyramidal mega-dune moved towards NE (35.97°) on the whole with a displacement distance of 0.29 m which was less than the shield dune in the same monitoring period. Although both the length and width of the mega pyramid dune decreased, the basal area, height and volume of the mega pyramid dune increased (Table 2, Figure 6). And the northern crestline of the pyramidal mega-dune migrated by approximately 3.44 m in the E direction, and the largest migration distance was 5.91 m, occurring in the middle of the crestline. The southeast crestline of the pyramidal mega-dune migrated by approximately 4.88 m in the NE direction, and the largest migration distance was 6.32 m, occurring at the bottom of the crestline. The middle part of the southwest crestline of the pyramidal mega pyramid dune migrated approximately by 3.59 m in the SE direction, while the movement of the other part of the crestline was not obvious.

The migration characteristic of the mega pyramid dune during 2015-2016 was almost the same as that in 2014-2015, and the movement direction was NE (59.9°) and the displacement was 0.4 m, which was less than those values of the

Table 2 Morphological parameters of the mega pyramid dune in different monitoring periods

Period	Length (m)	Width (m)	Height (m)	Basal area ($\times 10^4 \text{ m}^2$)	Volume ($\times 10^4 \text{ m}^3$)	Displacement (m)	Movement direction
2014	667.02	486.74	1238.76	10.58	200.37	0.29	NE 35.97°
2015	661.9	479.84	1240.14	10.61	202.11		
2016	670.3	481.2	1238.04	11.61	203.1	0.4	NE 59.9°

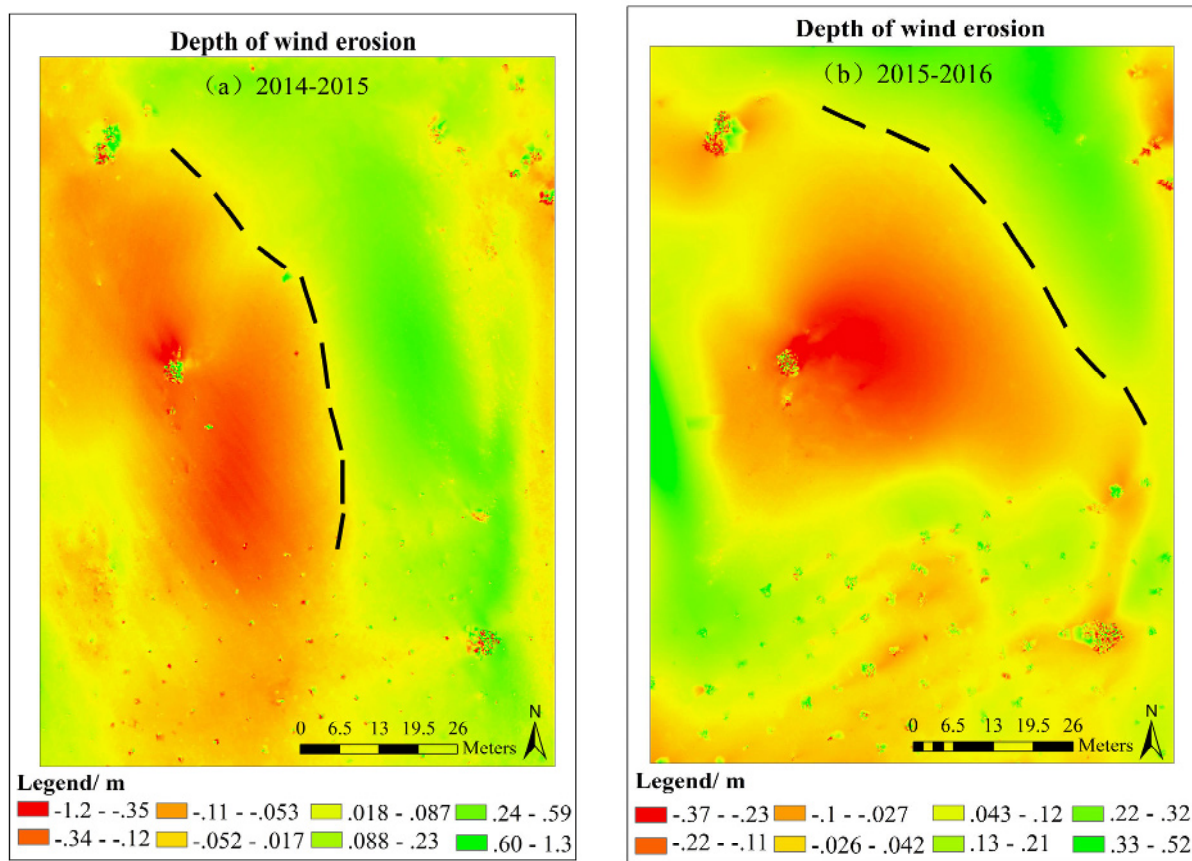


Figure 5 Dynamics of the monitored shield dune in the two monitoring periods. (a) 2014-2015; (b) 2015-2016. The dash line refers of the dune ridge of the monitored shield dune.

Table 3 Statistical data of aeolian erosion and deposition of the monitored mega pyramid dune

Year	Aspects	Erosion			Deposition			Total (+deposition;-erosion)	
		Mean (m)	Ration (%)	Volume ($\times 10^4 m^3$)	Mean (m)	Ration (%)	Volume ($\times 10^4 m^3$)	Volume ($\times 10^4 m^3$)	Unit area (m)
2014-2015	S	0.46	37.54	0.87	0.4	62.46	1.35	+0.48	0.08
	E	0.1	14.28	0.04	0.47	85.72	1.07	+1.03	0.39
	WNW	0.21	33.21	0.2	0.22	66.79	0.43	+0.23	0.08
	Total			1.11			2.85	+1.74	
2015-2016	S	0.25	36.8	0.35	0.19	63.2	0.79	+0.44	0.09
	E	0.17	42.1	0.19	0.35	57.9	0.78	+0.59	0.23
	WNW	0.14	73.3	0.21	0.22	26.7	0.17	-0.04	-0.11
	Total			0.75			1.74	+0.99	

Notes: the sign '+/-' in numbers of 'Total' represents deposition and erosion, respectively.

shield dune in the same monitoring period. The length, width, basal area and volume increased during the observation period, but the height decreased. Based on the above analysis, it was thus evident that the displacement of mega dune was less than the small dune. Both the basal area and volume increased in the two monitoring periods. Therefore, the mega pyramid dune increased in volume in the two years.

The monitored mega pyramid dune was mainly experiencing a deposition process in the monitoring period of 2014-2015, and aeolian erosion mainly occurred on the crestlines of the mega pyramid dune. Based on [Table 3](#) and [Figure 7a](#), the wind-erosion area accounted for approximately 37.54% of the S side and the average erosion depth was 0.46 m. The erosion mainly occurred on the dune surface near the crestline and

in the upper part of the S side. Comparatively, 62.46% (area proportion) of the S side experienced deposition and the average depositional thickness was approximately 0.4 m. The deposition mainly occurred at the bottom of the S side. The wind-erosion area of the E side accounted for approximately 14.28% and the average erosion depth was 0.1 m, while 85.72% of the E side experienced deposition and the average depositional thickness was approximately 0.47 m. The erosion also mainly occurred near the crestline, and the deposition mainly occurred at the bottom of the E side. Similarly, the wind erosion area of the WNW side accounted for approximately 33.21% and the average erosion depth was 0.21 m. The erosion mainly occurred at the bottom of the WNW side. Meanwhile, 66.79% of the WNW side experienced deposition and the average depositional thickness was approximately 0.22 m. The deposition mainly occurred on the dune surface near the crestline and in the upper part of the WNW side. Dune surface under wind erosion covered 30.59% of the total area of the entire dune surface, and the corresponding wind erosion amount reached $1.11 \times 10^4 \text{ m}^3$. Sand deposition took 69.41% in area, and the corresponding deposition amount was $2.85 \times 10^4 \text{ m}^3$. Thus, $1.74 \times 10^4 \text{ m}^3$ sands were deposited on the mega pyramid dune surface with an annual deposition rate of $0.16 \text{ m}^3 \cdot \text{m}^{-2} \cdot \text{yr}^{-1}$.

During 2015-2016 (Figure 7b), the area proportion of pyramid mega dune in deposition is more than that of erosion except the WNW side; for example, the area percentage on S side in

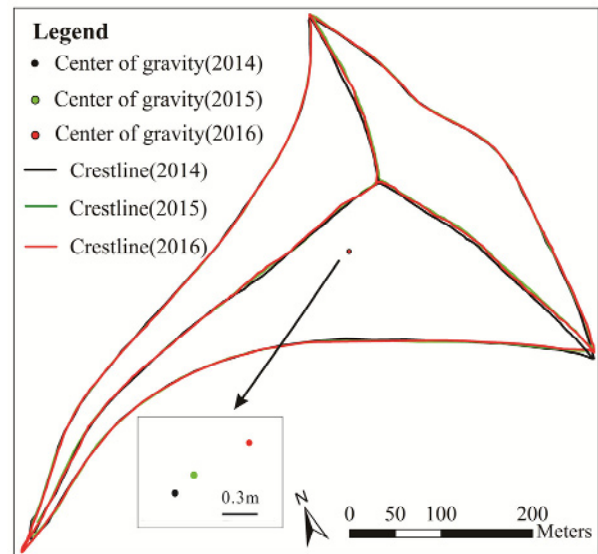


Figure 6 Variation of the morphology and the crestline of the monitored mega pyramid dune in the monitoring period.

deposition was 63.2% and that of erosion was just 36.8%. 36.65% of the total area of the entire dune surface was in erosion, and the corresponding wind erosion amount reached $0.75 \times 10^4 \text{ m}^3$. The dune surface in sand deposition took a percentage of 63.35%, and the corresponding deposition amount was $1.74 \times 10^4 \text{ m}^3$. Thus, $0.99 \times 10^4 \text{ m}^3$ sands were deposited on the mega pyramid dune surface with an annual deposition rate of $0.09 \text{ m}^3 \cdot \text{m}^{-2} \cdot \text{yr}^{-1}$.

According to the above analysis, it can be concluded that the volume of mega pyramid dune is increasing all the time and moves slower than

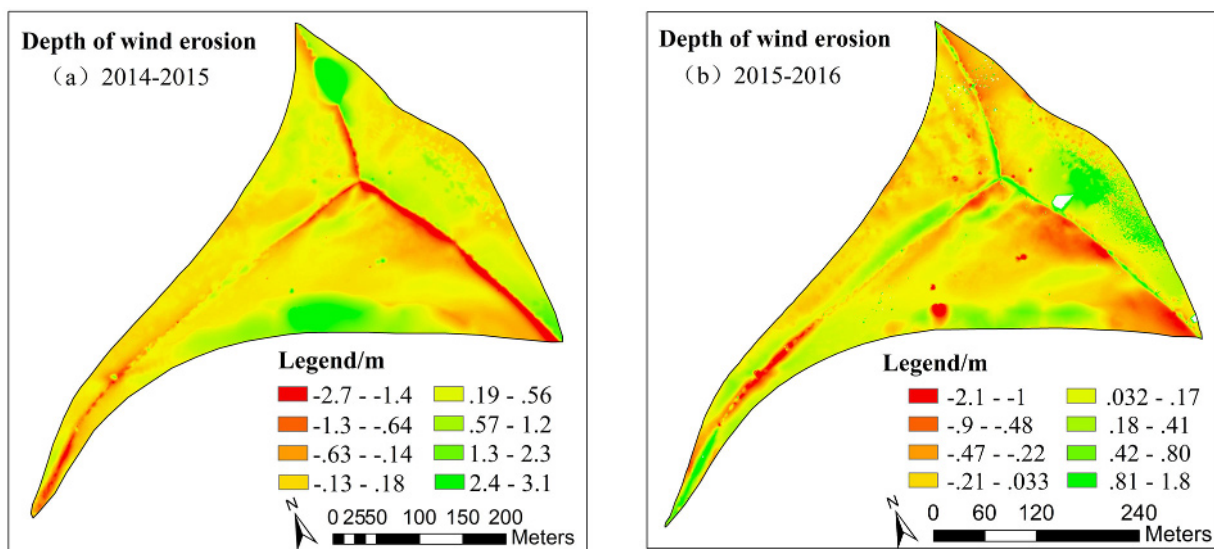


Figure 7 Dynamics of the monitored mega pyramid dune in the 2014-2015 (a) and 2015-2016 (b).

the shield dune, indicating that the monitored megadune plays a role of ‘sand container’ not a sand source for the Dunhuang Oasis compared with the shield dune. The volume of the shield dune is not only decreasing in all the monitoring periods, but also moves faster than the mega pyramid dune.

3 Discussion

At the edge of Dunhuang Oasis, in order to prevent the movement of dunes toward oasis or heritages, local government has settled integrated sand control systems such as engineering measures or alternative choice of building shelterbelts if the water is available (Qu et al. 2014; Zhang et al. 2016a). The engineering methods can fix some mobile dunes and partially cut the supply of sand materials. And shelterbelts, dominated by local psammophytes, also can obstruct the movement of dunes and improve soil condition in the meantime. Besides, much other vegetation has been planted in the area to increase surface roughness. However, the above sand control system has been built on dune surfaces of all types just according to the protective effect without considering the difference in dune dynamics. So as time goes on, many measures have failed gradually and the solution is continuing to establish new measures. But this way to protect the oasis will produce more disturbance to the fragile ecological environment and the protective effect was not prominent.

Our research shows that the displacement distance rate of the shield dune is larger than the mega pyramid dune on the southern edge of Dunhuang Oasis. Besides, our study indicates that the displacement distance is positively correlated to the dune length, width, height, basal area and volume. And the displacement distance has a negative correlation with the dune height. The higher the dune is, the less the displacement distance is (Tables 1 and 2).

By virtue of the faster migration speed, wind-blown sand supplemented by the shield dune will be further carried to the oasis, which is a threat to its survival. Such a process can be verified by the reduction of geometric feature parameters such as dune height and volume in the survey region as well as by results of erosion and deposition.

However, the mega pyramid dune increases in the volume in the monitoring period, playing a role of wind-blown sand “container” and also showing no migration. NW and NE are two prevailing wind directions in the study area, while S wind, a regional circulation, presents in the east of the study area, and thus the mega pyramid dune shows a relatively stable characteristic of dune dynamics affected by the above mentioned three wind directions. This also partially indicates that the development process of the monitored mega pyramid dune is of upward growth, and thus it is not a major sand supply for the Dunhuang Oasis compared with the shield dune. In view of this, we suggest that more attentions should be devoted to the control of shield dunes in the southern edge of Dunhuang Oasis.

4 Conclusions

In this paper, a 3-D laser scanner was used to study dune dynamics of a shield dune and mega pyramid dune at the southern edge of Dunhuang Oasis. Results indicate that the shield dune is shrinking while the mega pyramid dune is increasing in volume, and thus the mega pyramid dune actually serves as a “container” of wind-blown sand not as a major sand source. The movement rate of the gravity center of the shield dune is $2.85 \text{ m}\cdot\text{yr}^{-1}$; comparatively, that of the mega dune is $0.35 \text{ m}\cdot\text{yr}^{-1}$. Moreover, the shield dune decreases in volume and has an annual erosion rate of $0.02 \text{ m}^3\cdot\text{m}^{-2}\cdot\text{yr}^{-1}$ in the monitoring period; however, in contrast, the mega pyramid dune increases with an annual rate of $0.12 \text{ m}^3\cdot\text{m}^{-2}\cdot\text{yr}^{-1}$. Therefore, the shield dune will produce more threat to the oasis than the mega pyramid dune. And much more attention should be devoted from the control of mega dunes in the southern edge of Dunhuang Oasis to the control of shield dunes.

Acknowledgements

This research was supported by the National Natural Sciences Foundation of China (Grant No. 41871016), the National Key Research and Development Program of China (Grant No. 2017YFC0504801), Opening Fund of Key

Laboratory of Desert and Desertification, Chinese Academy of Sciences (Grant No. KLDD-2017-007) and Technology research and development

program of China Railway Urumqi Group Co., Ltd. (2017J002, 2017J003).

References

- Fryberger SG, Dean G (1979) Dune forms and wind regime. A Study of Global Sand Seas. U.S. Government Printing Office, Washington D.C. pp 137-169.
- Huang G, Qin X, He L, et al. (2015) Nonstationary desertification dynamics of desert oasis under climate change and human interference. *Journal of Geophysical Research Atmospheres* 120:11878-11888. <https://doi.org/10.1002/2015JD023826>
- Liu B, Zhang W, Qu J, et al. (2011) Controlling windblown sand problems by an artificial gravel surface: A case study over the gobi surface of the Mogao Grottoes. *Geomorphology* 134: 461-469. <https://doi.org/10.1016/j.geomorph.2011.07.028>
- Ma R, Wang J, Qu J, et al. (2010) Effectiveness of shelterbelt with a non-uniform density distribution. *Journal of Wind Engineering & Industrial Aerodynamics* 98: 767-771. <https://doi.org/10.1016/j.jweia.2010.07.001>
- Mao D, Lei J, Li SY, et al. (2014a) Differences of sand transportation flux and sand grain size characteristics in different underlying surfaces on desert-oasis ecotone in Cele. *Journal of Arid Land Resources & Environment* 28:167-174. (In Chinese).
- Mao D, Lei J, Zeng F, et al. (2014b) Sand Erosion and Deposition on Different Underlying Land Surfaces in the Desert-Oasis Ecotone in Cele, Xinjiang, China. *Journal of Desert Research* 34:961-969. (In Chinese)
- Pang YJ, Qu JJ, Zhang KC, et al. (2014) Quantitative analysis on the dynamic characteristics of megadunes around the Crescent Moon Spring, China. *Journal of Arid Land* 6: 255-263. <https://doi.org/10.1007/s40333-013-0245-0>
- Qu J, Cao S, Li G, et al. (2014) Conservation of natural and cultural heritage in Dunhuang, China. *Gondwana Research* 26: 1216-1221. <https://doi.org/10.1016/j.gr.2013.08.017>
- Heywood H (1942) The Physics of Blown Sand and Desert Dunes. p 68.
- Tan L, Zhang W, Qu J, et al. (2014) Variation with height of aeolian mass flux density and grain size distribution over natural surface covered with coarse grains: A mobile wind tunnel study. *Aeolian Research* 15: 345-352. <https://doi.org/10.1016/j.aeolia.2014.06.008>
- Tan L, Zhang W, Qu J, et al. (2016) Aeolian sediment transport over gobi: Field studies atop the Mogao Grottoes, China. *Aeolian Research* 21: 53-60. <https://doi.org/10.1016/j.aeolia.2016.03.002>
- Wang T, Xue X, Zhou L, et al. (2012) Combating Aeolian Desertification in Northern China. *Land Degradation & Development* 26: 118-132. <https://doi.org/10.1002/ldr.2190>
- Yong ZS, Wen ZZ, Pei XS, et al. (2007) Ecological effects of desertification control and desertified land reclamation in an oasis-desert ecotone in an arid region: A case study in Hexi Corridor, northwest China. *Ecological Engineering* 29: 117-124. <https://doi.org/10.1016/j.ecoleng.2005.10.015>
- Zhang K, An Z, Cai D, et al. (2016a) Key Role of Desert-Oasis Transitional area in Avoiding Oasis Land Degradation from Aeolian Desertification in Dunhuang, Northwest China. *Land Degradation & Development* 28:142-150. <https://doi.org/10.1002/ldr.2584>
- Zhang, K., Qu, J., Niu, Q., et al. (2013) Characteristics of wind-blown sand in the region of the Crescent Moon Spring of Dunhuang, China. *Environmental Earth Sciences* 70, 3107-3113. <https://doi.org/10.1007/s12665-013-2372-5>
- Zhang W, Qu J, Tan L, et al. (2016b) Environmental dynamics of a star dune. *Geomorphology* 273: 28-38. <https://doi.org/10.1016/j.geomorph.2016.08.005>
- Zhang W, Tan L, Zhang G, et al. (2014) Aeolian processes over gravel beds: Field wind tunnel simulation and its application atop the Mogao Grottoes, China. *Aeolian Research* 15: 335-344. <https://doi.org/10.1016/j.aeolia.2014.07.001>
- Zhang Z, Dong Z (2015) Grain size characteristics in the Hexi Corridor Desert. *Aeolian Research* 18: 55-67. <https://doi.org/10.1016/j.aeolia.2015.05.006>